論文 / 著書情報
Article / Book Information

Title	Development of Hiryu-II: A Long-Reach Articulated Modular Manipulator Driven by Thrusters
Authors	Yusuke Ueno, Tetsuo Hagiwara, Hiroyuki Nabae, Koichi Suzumori, Gen Endo
Citation	IEEE Robotics and Automation Letters, Vol. 5, Issue 3, pp. 4963 - 4969
Pub. date	2020, 6
Copyright	(c) 2020 IEEE. Personal use of this material is permitted. Permission from IEEE must be obtained for all other uses, in any current or future media, including reprinting/republishing this material for advertising or promotional purposes, creating new collective works, for resale or redistribution to servers or lists, or reuse of any copyrighted component of this work in other works.
DOI	https://dx.doi.org/10.1109/LRA.2020.3004775
Note	This file is author (final) version.

Development of Hiryu-II: A Long-reach Articulated Modular Manipulator Driven by Thrusters

Yusuke Ueno[1], Tetsuo Hagiwara[2], Hiroyuki Nabae[1], Koichi Suzumori[1], and Gen Endo[1]

***Abstract*—Robotic manipulators using thrusters for weight compensation are an active research topic due to their potential to exceed the limits of maximum length. However, existing manipulators that use thrusters have limitations of maximum length because the hardware design is not sufficiently refined. This paper focuses on overcoming these limitations and realizing an articulated manipulator more than twice the length of conventional ones. To cancel the moment for each link, we performed static analysis considering the torsional deformation around the link axis to derive the thruster position. Weight compensation and joint angle control of the manipulator can be realized with simple proportional integral derivative control for each link by numerical simulation. Consequently, we demonstrated the feasibility of the proposed manipulator by lifting a $0.6\ \mathrm{kg}$ payload at the arm end with a prototype of length $6.6\ \mathrm{m}$. Theoretically, each thrust force control input was almost constant, regardless of link attitude. This suggests modular properties that contribute to the practicality of the proposed manipulator for various tasks.**

***Index Terms*—Aerial Systems: Mechanics and Control, Redundant Robots, Cellular and Modular Robots, Field Robots**

I. INTRODUCTION

A long-reach articulated manipulator is required for various tasks, such as infrastructure inspection, decommissioning work for Fukushima Daiichi Nuclear Power Plants, and pesticide spraying in agricultural fields. In particular, if the manipulator is lightweight and modular, deployment to the site is easy, and the required length and payload can be adjusted according to various tasks. However, the development of a long-reach articulated manipulator presents a particularly difficult challenge.

The ultimate purpose of this study was to realize an extremely lightweight, long-reach, articulated manipulator that is modular, scalable, and practical on the ground. The target length and payload were 20- m-long and $5\ \mathrm{kg}$, respectively. Although some space manipulators[1][2] have the same length and are able to handle heavier payloads, their hardware design is simple and use conventional serial link chains because they are intended for operation in space, where gravity is very small. By contrast, gravity is much greater on the ground; therefore, the most critical limitation of a long-reach manipulator is compensating for the weight of the super long-reach manipulator. Although there are various methods, such as using a telescopic mechanism like a crane supported by a structure, using a wire drive mechanism[3][4], using a spring[5][6][7][8][9], or using buoyancy[10][11], they are all difficult to realize modularly for high payloads. For example, a telescopic mechanism is large and heavy, which makes it inconvenient. The specifications of the wire drive mechanism cannot be adjusted owing to its complexity. The spring is too heavy to assist the slender manipulator, and, depending on the payload, the compensation torque is difficult to adjust. Moreover, buoyancy cannot be applied to high payloads.

To overcome this problem, we adopted thrusters for the weight compensation of the manipulator[12]. Assuming that there is no limitation for energy source, we can achieve the above goal by placing each thruster at an appropriate position and controlling the thrust force. Some studies have adopted water jets as thrusters[13][14][15]. However, it is difficult to obtain a sufficient jet for weight compensation because water is heavy, which limits the maximum length of the manipulator. If we choose propellers driven by electric motors, we can easily realize a modular system with great length by connecting the power cable in a "daisy chain".

Related work is LASDRA[16], which also drives joints with propellers. LASDRA[16] requires eight propellers for each link due to the purpose of generating a three-axis force at a spherical joint with propeller thrust force[17], which means that only few actuators contribute to the weight compensation. Therefore, the maximum length of the manipulator is also limited in this case. Compared to this, in our previous work, Hiryu-I[12], we introduced a parallel link mechanism so that the thruster always follows the direction of gravity, aiming at a more practical and simple system. Thanks to the parallel link mechanism, the thrust force can be constant without depending on the link attitude, and its control can be remarkably simplified.

In Hiryu-I[12], a thruster was installed only in the direction of gravity to cancel gravity with thrust force, and an electric servomotor on the swivel axis was used for horizontal rotation. We succeeded in controlling the end position in three-dimensional space with three units prototype of length $3\ \mathrm{m}$.

Manuscript received: February, 24, 2020; Revised May, 22, 2020; Accepted June, 14, 2020.

This paper was recommended for publication by Editor Jonathan Roberts upon evaluation of the Associate Editor and Reviewers' comments. *This work was supported by the New Energy and Industrial Technology Development Organization (NEDO). This work was also supported by JSPS KAKENHI, Grant Number JP18K04044.

[1]Yusuke Ueno, Hiroyuki Nabae, Koichi Suzumori, and Gen Endo are with the Department of Mechanical Engineering, Tokyo Institute of Technology, 2-12-1 Ookayama, Meguro-ku, Tokyo 152-8550, Japan ueno.y.ah@m.titech.ac.jp

[2]Tetsuo Hagiwara is with Yokohama KH Tech Corporation, 1-22-14 Kaminakatani, Konan-ku, Yokohama, Kanagawa 233-0012, Japan hagiwara@ykh-tech.co.jp

Digital Object Identifier (DOI): see top of this page.

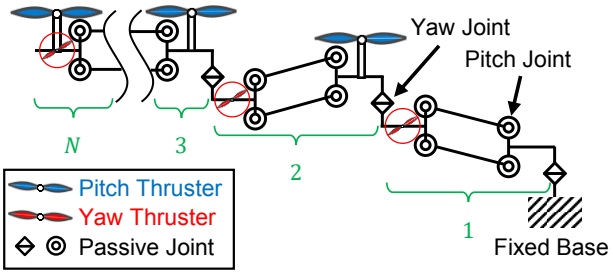

Fig. 1. Mechanism of the proposed manipulator. Of the N parallel links, we define the most proximal as 1-st unit, and the most distal as N-th unit.

However, when we extended the link and made the total length 5 m, torsional deformation around the link axis caused excessive torque against the swivel actuator and could not achieve the stable position control. Thus, Hiryu-I[12] had a maximum length limitation. In addition, its mass was increased due to installation of the servomotor on the link.

The purpose of this study was to address and propose solutions to the aforementioned problems. The main contribution of this paper is the realization of a prototype that is more than twice the length of conventional thruster-assisted manipulators. Another important contribution is the proposal of a solution to the electrical cable weight problem for realizing a larger manipulator. To achieve this goal, we propose Hiryu-II, which also drives the swivel joint with a thruster. Even with a small drive thruster in the swivel direction, a sufficiently large swivel torque can be generated due to the placement at the arm end. Next, to cancel the moment for each link, we performed static analysis considering the torsional deformation around the link axis to derive the thruster position. Weight compensation and joint angle control of the manipulator were realized with simple proportional integral derivative (PID) control for each link by numerical simulation. Finally, we showed that the proposed method can realize a prototype more than twice the length of a conventional long-reach articulated manipulator.

II. PROPOSED SYSTEM

In this section, we propose a long-reach articulated modular manipulator (Hiryu-II) in which all joints are passively driven by thrusters, in addition to the basic features of Hiryu[12] proposed by our research group. Each joint is passive and does not include an actuator.

Figure 1 shows the configuration of Hiryu-II. A parallel link mechanism consisting of pitch passive joints is serially connected with yaw passive joints. We adopt a fixed pitch propeller as a thruster for simplicity. Since the yaw thruster is located at the distal end of the long parallel link, the torque around the proximal yaw joint becomes sufficiently large.

Hiryu-II is also safer than conventional multicopters because these mechanical constraints limit the range of motion. One application of Hiryu-II is an infrastructure inspection system that performs observations and hammering tests while utilizing its redundancy for obstacle avoidance.

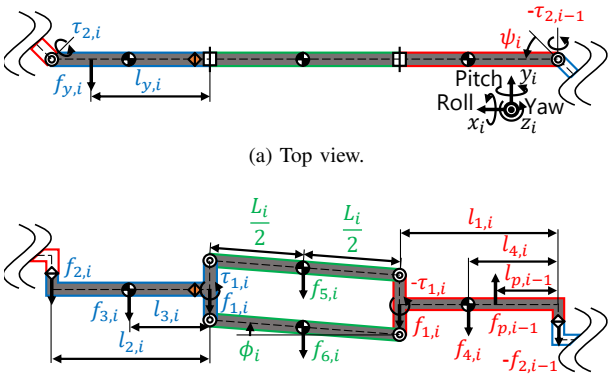

(a) Top view.

(b) Front view.

Fig. 2. Kinematic model for i-th unit ($1 \leq i \leq N-1$). $f_{1,i}, f_{2,i}$ and $\tau_{1,i}, \tau_{2,i}$ represent internal force and internal torque, respectively. $f_{3,i}, f_{4,i}, f_{5,i}, f_{6,i}$ represent the gravity of the links, and $f_{\mathrm{p},i}$, $f_{\mathrm{y},i}$ represents the thrust force. ϕ_i is pitch and ψ_i is yaw.

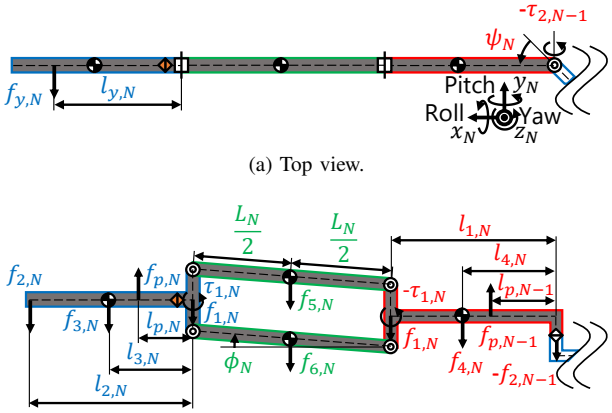

(a) Top view.

(b) Front view.

Fig. 3. Kinematic model for N-th unit.

III. SYSTEM MODELING

In this section, we reflect the deformation of the proposed manipulator by a kinematic model. We approximated a flexible manipulator using multiple virtual rigid links and virtual passive joints including springs and dampers. A similar method was applied in the research of the AIA Robot[6].

A. Problem Setting

Figure 2 and Figure 3 show the physical parameters for the i-th unit ($1 \leq i \leq N-1$) and the N-th unit, respectively. Virtual roll axis passive joints are introduced to compensate for torsional deformation by considering the static balance of force and moment. The equilibrium points of the virtual roll axis passive joints are in the horizontal posture. In the analysis, we define a body with weight $f_{3,i}$ as the front link, a body with weight $f_{4,i}$ as the rear link, a body with weight $f_{5,i}$ as the upper link, and a body with weight $f_{6,i}$ as the lower link. We also assume a payload f_{load} on the arm end. Σ_i is the coordinate system fixed to the i-th unit.

As shown in Fig. 2a and Fig. 3a, we regard gravitational torque propagation to the base as the most dominant influ-

encing factor of torsional deformation. We are interested in solving this problem while achieving the independence of each joint angle control. This policy is derived from the advantage of the modular structure of Hiryu-II. The definition of joint angle control independence is as follows: the thrust force, which is the control variable, is determined by only one local joint angle feedback. Therefore, in the next section, we discuss the design of the manipulator that achieves torsional deformation compensation and independence of each joint angle control.

B. Determination of Thruster Position

Based on static analysis, we examine the issues of thruster position arrangement. The goal of optimization is as follows: any gravitational torque $\tau_{2,i}$ (the dependent variable of weight, length, and joint angle) does not depend on any joint angle ϕ_j, $\psi_j\,(1 \leq j \leq N)$ (independent variables). To achieve this goal, we assume that any gravitational torque $\tau_{2,i}$ is an independent variable and explain the dependency of thruster position $l_{\mathrm{p},i}$ on the weight and length. The equilibrium of the moment around the virtual roll passive joint of the front link is given by the identity for the yaw joint angle ψ_{i+1}, as shown in (1).

$$\begin{aligned} {}^{i}\boldsymbol{e}_x \cdot {}^{i}\boldsymbol{R}_{i+1}\,{}^{i+1}\boldsymbol{\tau}_{2,i} &= \tau_{1x,i}\cos\psi_{i+1} + \tau_{1y,i}\sin\psi_{i+1} \\ &= \left|{}^{i+1}\boldsymbol{\tau}_{2,i}\right|\sin\left(\psi_{i+1}+\alpha\right) \\ &= 0 \end{aligned} \tag{1}$$

$${}^{i}\boldsymbol{e}_x = \begin{pmatrix} 1 & 0 & 0 \end{pmatrix}^T \tag{2}$$

$${}^{i}\boldsymbol{R}_{i+1} = \begin{pmatrix} \cos\psi_{i+1} & \sin\psi_{i+1} & 0 \\ -\sin\psi_{i+1} & \cos\psi_{i+1} & 0 \\ 0 & 0 & 1 \end{pmatrix} \tag{3}$$

$${}^{i+1}\boldsymbol{\tau}_{2,i} = \begin{pmatrix} \tau_{2x,i} & \tau_{2y,i} & 0 \end{pmatrix}^T \tag{4}$$

where ${}^{i}\boldsymbol{e}_x \in \mathbb{R}^3$ is a unit vector, ${}^{i}\boldsymbol{R}_{i+1} \in \mathbb{R}^{3\times3}$ is a rotation matrix from Σ_{i+1} to Σ_i, and ${}^{i+1}\boldsymbol{\tau}_{2,i} \in \mathbb{R}^3$ is the gravitational torque acting on the passive joint around z_i. The components of ${}^{i+1}\boldsymbol{\tau}_{2,i}$ are expressed as in (4). The upper left subscript indicates the reference coordinate system of the vector. For example, ${}^{i+1}\boldsymbol{\tau}_{2,i}$ is expressed in Σ_{i+1}. $\alpha \in \mathbb{R}$ is a constant. Therefore, if the thruster position satisfies (5), we can compensate for the torsional deformation under static conditions.

$$\left|{}^{i+1}\boldsymbol{\tau}_{2,i}\right| = 0 \tag{5}$$

Based on the assumption of (5), the internal force $f_{1,i}$ between the front link, upper link, and lower link is given by (6).

$$f_{1,i} = \frac{1}{2}\sum_{k=5}^{6} f_{k,i} \quad (1 \leq i \leq N) \tag{6}$$

Solving the equation for the z_i axial force acting on the front link, we find that the internal force $f_{2,i}$ is constant regardless of the joint angle, as shown by (7).

$$f_{2,i} = \begin{cases} -\left(f_{1,i} + f_{3,i}\right) & (1 \leq i \leq N-1) \\ f_{\mathrm{load}} & (i = N) \end{cases} \tag{7}$$

TABLE I. Parameters used for the dynamic analysis of the three units model. The parameters of link weight were measured for the three units prototype (including the electric cable), and the parameters of dimension were obtained from numerical calculation with 3D-CAD. Note that the weight of electric cable does not contribute to the center of gravity position of the link, because we added it as a mass point to the center of gravity.

i	1	2	3
$f_{3,i}$ [N]	5.27	5.22	16.2
$f_{4,i}$ [N]	16.8	27.2	26.3
$f_{5,i}$ [N]	4.81	3.82	2.83
$f_{6,i}$ [N]	4.81	3.82	2.83
$l_{1,i}$ [mm]	643	643	643
$l_{2,i}$ [mm]	35.5	35.5	26.5
$l_{3,i}$ [mm]	58.6	58.6	25.0
$l_{4,i}$ [mm]	364	323	326
$l_{\mathrm{p},i}$ [mm]	274	281	7.5
$l_{\mathrm{y},i}$ [mm]	143	143	143
L_i [mm]	1513	1513	1513

Next, we solve the equation for the z_i axial force acting on the rear link. As a result, we obtain (8), which gives the weight compensation force $f_{\mathrm{p},i}$ for thrusters.

$$f_{\mathrm{p},i} = \begin{cases} f_{1,i+1} + f_{4,i+1} - f_{2,i} & (1 \leq i \leq N-1) \\ f_{1,N} + f_{3,N} & (i = N) \end{cases} \tag{8}$$

Our proposed method satisfies the independence of each joint angle control because the equation does not include any joint angles. When we apply this method to a prototype, we can automatically optimize the thrust force through integral control of the pitch joint angle.

Furthermore, the gravitational torque $\tau_{1,i}$ between the front link, upper link, and lower link can be expressed by (9).

$$\tau_{1,i} = \begin{cases} -\displaystyle\sum_{k=2}^{3} l_{k,i} f_{k,i} & (1 \leq i \leq N-1) \\ l_{\mathrm{p},N} f_{\mathrm{p},N} - \displaystyle\sum_{k=2}^{3} l_{k,i} f_{k,i} & (i = N) \end{cases} \tag{9}$$

Finally, we consider the equation of moment around the z_i axis of the rear link. The thruster position $l_{\mathrm{p},i}$ under the assumption of (5) can be determined by (10).

$$l_{\mathrm{p},i} = \begin{cases} \dfrac{1}{f_{\mathrm{p},i}} \displaystyle\sum_{k=1}^{4} l_{k,i+1} f_{k,i+1} & (1 \leq i \leq N-2) \\ \dfrac{l_{\mathrm{p},N} f_{\mathrm{p},N} + \displaystyle\sum_{k=1}^{4} l_{k,N} f_{k,N}}{f_{\mathrm{p},N-1}} & (i = N-1) \\ l_{\mathrm{p},N} & (i = N) \end{cases} \tag{10}$$

where $l_{\mathrm{p},N}$ is an independent variable. $l_{\mathrm{p},i}$ is also independent of all joint angles. This suggests that there is an appropriate thruster position that can completely compensate for the torsional deformation of the structure due to the static load for any posture of the proposed manipulator.

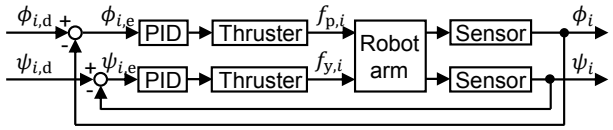

Fig. 4. Control block diagram of joint angles ϕ_i and ψ_i. $\phi_{i,\mathrm{d}}$ and $\psi_{i,\mathrm{d}}$ are target joint angle values. $\phi_{i,\mathrm{e}}$ and $\psi_{i,\mathrm{e}}$ are angle deviations.

TABLE II. Parameters adjusted by the PID controller for each joint angle. f is the cutoff frequency of the first-order low-pass filter of the differentiator. The control cycle was set to 400 Hz.

Target	ϕ_1	ϕ_2	ϕ_3	ψ_1	ψ_2	ψ_3
K_p [N/deg]	0.45	0.30	0.15	0.080	0.050	0.025
K_i [N/(deg·s)]	0.04	0.02	0.01	0.005	0.003	0.001
K_d [N/(deg/s)]	0.12	0.08	0.04	0.20	0.10	0.05
f [Hz]	20	20	20	100	100	100

C. Dynamic Analysis

In this section, we analyze the manipulator dynamics for two purposes: to confirm the feasibility of position control of the pitch joint for the determined thruster position and to confirm the feasibility of position control of the yaw joint proposed in Section II. We adopted MATLAB Simscape Multibody for simulation. In the analysis model, the spring constant and damper constant of the virtual roll axis passive joint were assumed to be 0.89 Nm/deg and 0.05 Nm/(deg/s), respectively. Other parameters were set as listed in Table I. Figure 4 shows the control block evaluated by dynamic analysis. We performed PID control of all joint angles independently for each unit. Thereafter, we adjusted each PID gain heuristically and adopted the parameters listed in Table II. We set the initial integral term of the pitch PID controller to the value obtained from (8) and Table I and set the term of the yaw PID controller to 0.

Figure 5a and Figure 5b correspond to the joint angle and time history of thrust force, respectively. Both of them are the results obtained by dynamic analysis. We have given a target angle that changes like a trapezoid, as shown in Fig. 5a. The initial joint angles were set as $\phi_i = \phi_{i,\mathrm{d}} = 0$ and $\psi_i = \psi_{i,\mathrm{d}} = 0$. We confirmed that the control variable $f_{\mathrm{p},i}$ takes an almost constant value for various arm postures, as shown by (8), although it fluctuates from 15 s to 25 s and from 45 s to 55 s due to acceleration/deceleration and contact force between the units, respectively. In other words, thrust force is almost constant owing to the parallel link mechanism, and the position control of the pitch joint is remarkably easy. We also succeeded in tracking the target angle under the influence of disturbance by setting the appropriate parameters for position control of the yaw joint. Interestingly, we noticed that $f_{\mathrm{y},i}$ has a long moment arm of 2300 mm, therefore only a small amount of power can be fully actuated under ideal conditions. This contributes to a reduction in the proportion of actuator weight in the manipulator.

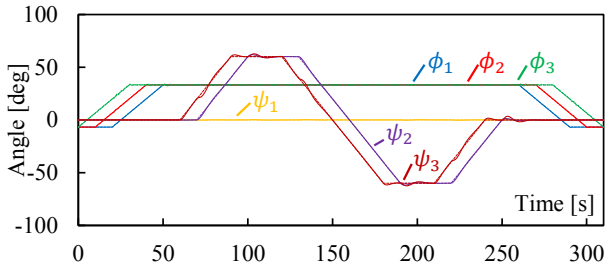

(a) Time history of joint angles. The solid line represents the analysis result, and the broken line represents the target value.

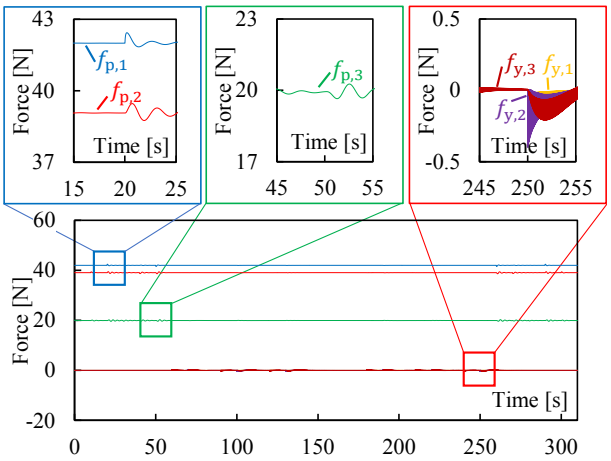

(b) Time history of the thrust force.

Fig. 5. Result of dynamic analysis with three units model.

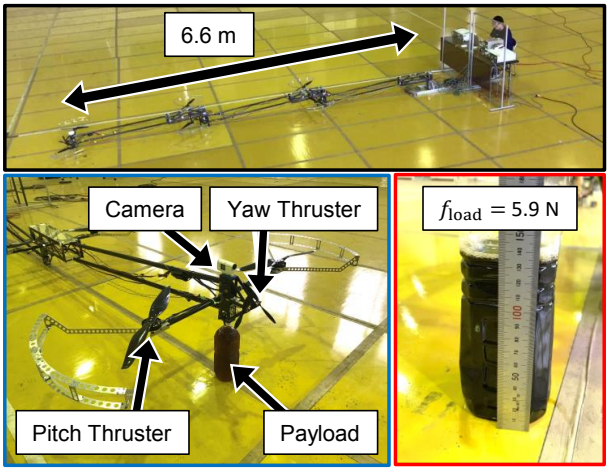

Fig. 6. Prototype "Hiryu-II 6.6 m Model" (black). Enlarged view of the arm end (blue). Payload used in experiment 2 (red).

IV. PROTOTYPE OVERVIEW

To confirm the principle of weight compensation and joint drive mechanism by thrusters, we developed a three units prototype named "Hiryu-II 6.6 m Model". In this section, we introduce its design comprehensively.

The prototype can be roughly divided into two parts: manipulator and base. Table III lists the specifications of the manipulator. The mass is the measured value including the weight of the electric cable. Other values, except for mass, were analyzed

TABLE III. Specifications of "Hiryu-II 6.6 m Model".

Length (horizontally extended)	6575 mm
Width	1470 mm
Mass	16.2 kg
	(Arm:12.2 kg, Base:4.00 kg)
Payload (at arm end)	6.87 kg
Power Consumption	2000 W
(at static posture, payload 0 kg)	
Range of Motion	ϕ_i : ±48 deg
	ψ_i : ±180 deg

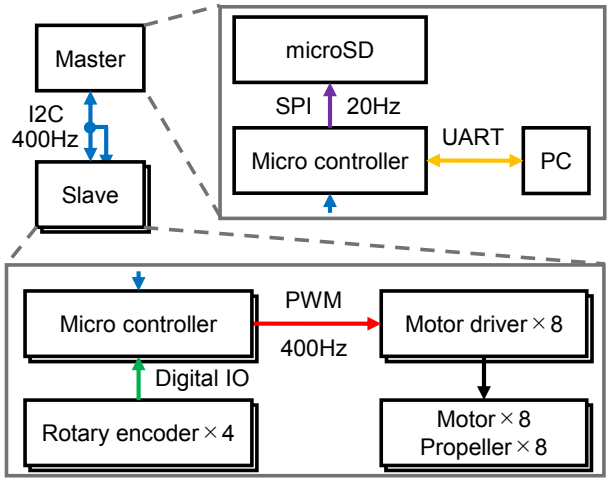

Fig. 7. System configuration of the prototype. Each slave can control 4 DoF, which is equivalent to two units. In the experiment, we used one master and two slaves.

from a 3D-CAD model of the manipulator. We used power cables and signal cables with densities of 2.79×10^{-2} kg/m and 5.55×10^{-3} kg/m, respectively. The parallel link consisted of two carbon fiber reinforced polymer pipes with outer diameters of 25 mm and thicknesses 1 mm. All joints were freely rotatable and driven passively by thrusters. The thrusters for pitch angle control consisted of a propeller (TL2845, TAROT) with diameter 0.508 m, pitch 0.140 m, and a motor (6008, TAROT) with a maximum power of 637 W and a motor driver (FlyDragon V1-60A, FLYCOLOR), each with 43.2 N maximum thrust force. The thrusters for yaw angle control also consisted of a propeller (PP228, KK HOBBY) with diameter 0.203 m, pitch 0.0965 m, and a motor (BE1806, DYS) with a maximum power of 79.9 W and a motor driver (Multistar 10A V2, Turnigy), each with 4.31 N maximum thrust force. On each unit, we installed two thrusters for weight compensation rotating in opposite directions to cancel the counter torque generated by rotation. We also installed two thrusters for yaw angle control in each unit to support forward and reverse rotation. We designed the parallel link mechanism offset from the yaw joint to obtain a wide range of motion, as shown in Table III.

The base contained a circuit board for operation and had a mass of 4.0 kg. Figure 7 shows the system configuration of the prototype. The thrust force of each unit is controlled by a simple PID controller, as shown in Fig. 4.

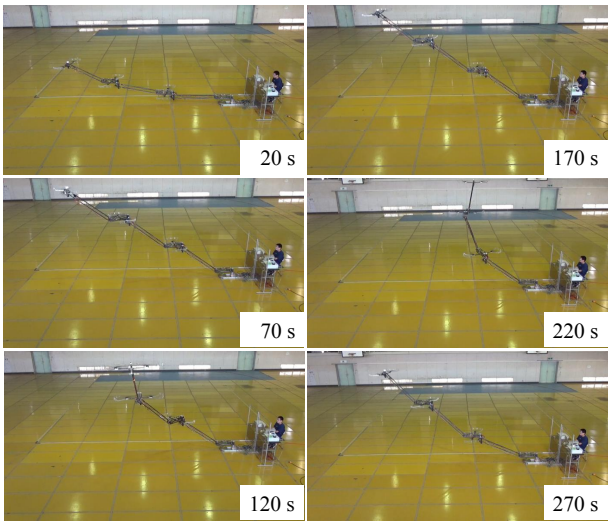

(a) Snapshot of the experiment. Time corresponds to the horizontal axes in Fig. 8b and Fig. 8c.

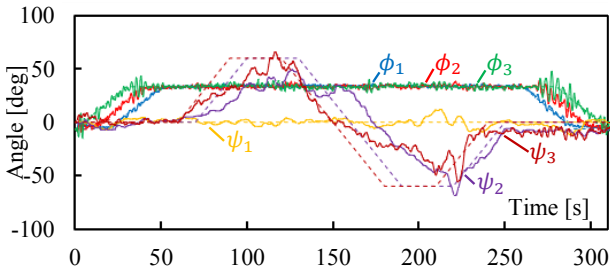

(b) Time history of joint angles. The solid line represents the experimental results, and the broken line represents the target value.

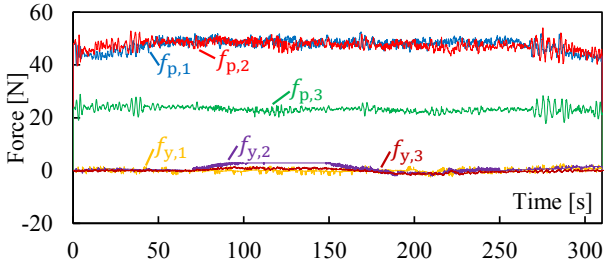

(c) Time history of thrust force. In a preliminary experiment, we recorded the PWM input signal to the motor driver and the output signal of the force sensor corresponding to the thrust force. The rotation speed of the motor that generates thrust force is linear to the PWM input signal of the motor driver. From the rotor blade theory, we approximated the thrust force through the motor rotation speed, that is, the second-order polynomial of the PWM input signal. In this experiment, we estimated the time history by recording the PWM input signal instead of the thrust force for simplicity. Therefore, it should be noted that we did not actually measure the thrust force during operation.

Fig. 8. Results of Experiment 1 with three units prototype.

V. EXPERIMENTAL RESULTS

In this section, we report the evaluation results of the basic motion of Hiryu-II. We performed the experiment in an indoor environment capable of supplying 6000 W power. We installed a weight (approximately 40 kg in total) on the base to prevent rollover. We gradually proceeded with the experiment while extending the prototype from one unit to three units. In the experiment of the one unit prototype, we

TABLE IV. RMS of each joint angle obtained from Experiment 1 with three units prototype

Target	$\phi_{1,\mathrm{e}}$	$\phi_{2,\mathrm{e}}$	$\phi_{3,\mathrm{e}}$	$\psi_{1,\mathrm{e}}$	$\psi_{2,\mathrm{e}}$	$\psi_{3,\mathrm{e}}$
RMS [deg]	1.41	2.18	3.09	3.88	16.1	15.6

set the PID gain as shown in the third and sixth columns of Table II, and confirmed that it consumed 180 W for weight compensation. Then, we added the proximal parallel link module while keeping the PID gains of the distal links, and set their PID gains as shown in the second and fifth columns of the Table II. In terms of power consumption, the two units prototype required 900 W for weight compensation. And in the assembly of the three units prototype, the parameters of each link in 1-st, 2-nd, and 3-rd unit were approximately equal to those in Table I. We also set the PID gain with reference to Table II.

A. Basic Motion with No Payload (Experiment 1)

We used the three units prototype for Experiment 1 to confirm the basic motion of Hiryu-II. Figure 8a shows a snapshot of the experiment. Figure 8b and Figure 8c show the time history of the joint angle and thrust force, respectively. We lifted the manipulator and turned it left and right, as shown in Fig. 8a.

We defined the pitch joint as the absolute angle with the horizontal attitude 0 deg and the yaw joint as the relative angle with the proximal link. Table IV shows the RMS of the angular deviation during Experiment 1. For pitch joints, we confirmed the contribution of the PID controller to changes in target angle. The thrust force $f_{\mathrm{p},i}$ was almost constant, as shown by (8), and was independent of any joint angle. This indicates that the design concept proposed in Section III includes the advantage of selecting a thruster that matches the mass characteristics of the manipulator. Although the angle deviation remained, the yaw joint was stable. We consider that the displacement of the thrust vector due to the slight torsional deformation of the mechanical structure affected the enlargement of the deviation. This is implied from the fact that the system is stable even when the thrust force $f_{\mathrm{y},i}$ is saturated from 100 s to 150 s. Thrust force saturation occurs because the motor is controlled not to exceed the maximum performance. If deformation of the manipulator is tolerable, the introduction of a higher power thruster is one possible improvement. The power consumption required for operation was approximately 2000 W at equilibrium.

B. Lifting 0.6 kg Payload (Experiment 2)

Next, we performed Experiment 2 to confirm the robustness of the manipulator with a payload of 0.6 kg at the arm end. PID gain was set as in Table II. Figure 9a shows a snapshot of the experiment. Figure 9b and Figure 9c show the time history of the joint angle and thrust force, respectively.

For the sake of simplicity, we kept the target angles of all the yaw joints constant at 0 deg during the experiment. However, we frequently observed a phenomenon in which the deviation of the joint angle increased in the negative direction

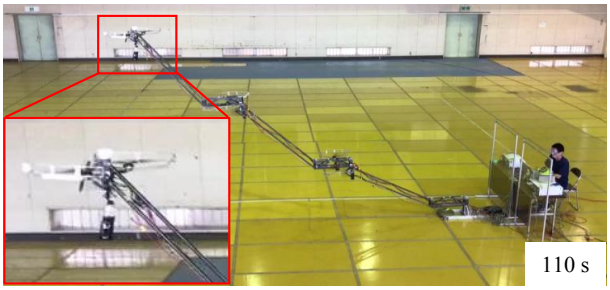

(a) Snapshot of Experiment 2.

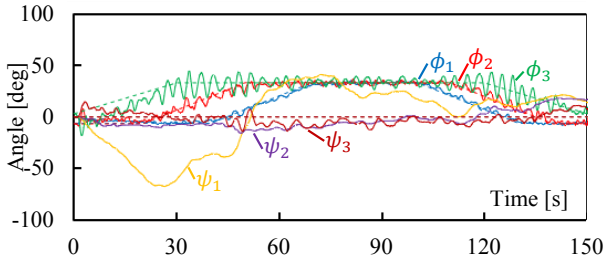

(b) Time history of joint angles. The solid line represents the experimental results, and the broken line represents the target value.

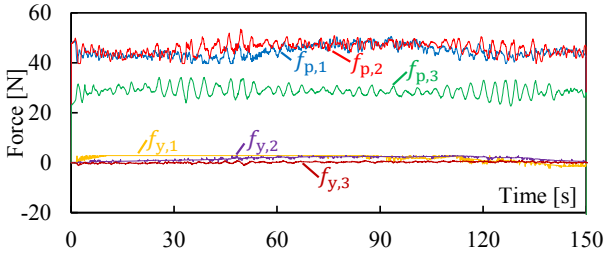

(c) Time history of thrust force. Note that we did not actually measure the thrust during operation, but we estimated it from the log data of the input signal.

Fig. 9. Results of Experiment 2 with three units prototype.

at the beginning of the experiment. It is likely that installation error was a factor causing this problem. Compared to Fig. 8b and Fig. 8c, the pitch joint angle ϕ_i and the thrust force $f_{\mathrm{p},i}$ became oscillatory. Nevertheless, it should be noted that, under constrained conditions, the same PID controller can handle, to some extent, the gravitational force disturbances induced by the payload. The time average of the thrust force $f_{\mathrm{p},3}$ increased by 5.18 N, corresponding to the payload $f_{2,3}$ in total. The power consumption at equilibrium also increased by approximately 100 W.

C. Expansion to Four units Prototype (Experiment 3)

Finally, we extended the prototype to four units (8.8 m in total) and confirmed its feasibility experimentally. The assembly was successful. However, when installed on the ground, the strength of the fasteners between the yaw joint shaft and the link was insufficient due to the effect of the huge gravitational torque. We managed to perform a control experiment because the gravitational torque would be compensated for once it ascended. As shown in Fig. 10, we succeeded in lifting the 8.8- m-long manipulator directly upwards.

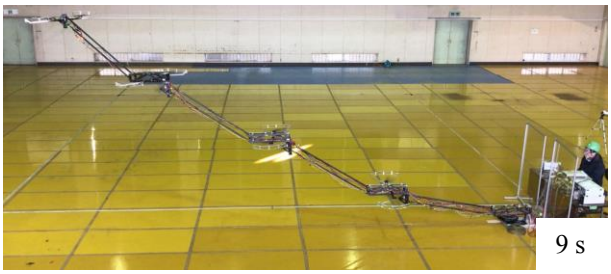

Fig. 10. Snapshot of the moment when the four units prototype was lifted successfully in Experiment 3. We set the desired joint angles as $(\phi_{1,\mathrm{d}}, \phi_{2,\mathrm{d}}, \phi_{3,\mathrm{d}}, \phi_{4,\mathrm{d}}) = (t - 6.2, 30, 30, 30)$ and $(\psi_{1,\mathrm{d}}, \psi_{2,\mathrm{d}}, \psi_{3,\mathrm{d}}, \psi_{4,\mathrm{d}} = (0, 0, 0, 0))$.

However, joint angles were difficult to control. We believe that this problem stems from the accumulation of dimensional errors (especially in the thruster position) of the prototype. Some possible measures to remedy this include adjusting the thruster position and PID gain based on the behavior of the prototype and damping each unit with inertial measurement unit (IMU) and thrusters.

VI. DISCUSSION

In the experimental results presented in Section V, we observed random torsional deformation around the roll axis. This causes the following two problems. First, the end position accuracy is reduced. Even a slight torsional deformation manifests as a large deviation at the arm end. Second, the control performance of joint angles is reduced. If the rotational axis of the passive joint does not match the direction of the thrust vector for driving the joint, the desired control performance cannot be obtained. We were able to confirm that the control performance of the yaw axis reduced. This is related to the aforementioned problem of the poor end position accuracy. To address the issue of random torsional deformation, balancing the roll direction with two thrusters for weight compensation could be an effective solution. Considering its conventional role, the sum of the thrust force of the two thrusters corresponds to the driving force of the pitch joint, and the difference of the thrust force corresponds to the roll direction balancer. The IMU is suitable for calculating the torsional deformation. Motion capture can be used to evaluate any subsequent improvement in the end position accuracy.

In Experiment 2, Section V, it could be observed that the manipulator could operate, to some extent, with the PID controller that was used in Experiment 1. By contrast, we have to deal with oscillations of the joint angle and thrust forces. In cases where the payload is known, we consider that readjustment of the gain is effective.

With the current hardware design, it is possible to realize a four units prototype; however, to make the manipulator longer, it is necessary to reduce the weight of electric cables. In this case, we have 10 power cables with a density of 2.79×10^{-2} kg/m and 52 signal cables with a density of 5.55×10^{-3} kg/m. In terms of weight, the most distal link is 3.45 N (of which 25.9% corresponds to the signal cables), whereas the most proximal link is 11.9 N (of which 49.4% corresponds to the signal cables). When expressed as a percentage of the total link weight of each module (32.9 N), they are 10.5% and 36.1%, respectively. Therefore, in contrast to that in the most distal links, the number of electrical cables in the most proximal links is enormous, and their weight is not negligible, which causes frictional resistance of the joint and limits the maximum length of the manipulator. A possible solution to this problem is to disperse the circuit boards on the manipulator and reproduce the equivalent system. For simplicity, all circuit boards in the prototype were placed on the base; however, the 52 signal cables for controlling the actuator became long, resulting in a weight increase of 17.8% of the total link weight at the most proximal link. By reducing only one cable for communication between MCUs, instead of 52 signal cables for actuator control, or making it wireless, we can distribute the circuit boards, and, consequently, reduce the weight of the signal cables. Although there are fundamental restrictions on power cables, signal cables are modular; therefore, the possibility of realizing a larger manipulator still exists.

VII. CONCLUSIONS

In this paper, we proposed a super long-reach articulated modular manipulator named Hiryu-II that performs weight compensation and joint drive with thrusters. We proposed a method that satisfies the weight compensation and independence of each joint angle control at the same time by focusing on the torsional deformation generated in the manipulator. The feasibility of the manipulator was demonstrated by basic control experiments on a three units prototype (6.6 m in total) and four units prototype (8.8 m in total).

In the future, we plan to (1) measure the torsional deformation of each unit and the three dimensional position of the arm end quantitatively, (2) conduct several experiments with various motion profiles to assess the performance of the proposed manipulator quantitatively, (3) implement end effector force control, which is associated with our previous work[18], (4) conduct experiments and analyses lifting heavy payloads assuming disturbances in the outdoor environment, and (5) improve the prototype and expand to four units with a total length of 20 m.

ACKNOWLEDGMENT

This paper is based on the results obtained from a project commissioned by the New Energy and Industrial Technology Development Organization (NEDO). This work was also supported by JSPS KAKENHI Grant Number JP18K04044.

REFERENCES

[1] C. Sallaberger, "Canadian space robotic activities," *Acta Astronautica*, vol. 41, no. 4, pp. 239 – 246, 1997. [Online]. Available: http://www.sciencedirect.com/science/article/pii/S0094576598000824

[2] R. Boumans and C. Heemskerk, "The european robotic arm for the international space station," *Robotics and Autonomous Systems*, vol. 23, no. 1, pp. 17 – 27, 1998. [Online]. Available: http://www.sciencedirect.com/science/article/pii/S0921889097000547

[3] A. Horigome, G. Endo, K. Suzumori, and H. Nabae, "Design of a weight-compensated and coupled tendon-driven articulated long-reach manipulator," *2016 IEEE/SICE International Symposium on System Integration (SII)*, pp. 598–603, 2016.

[4] G. Endo, A. Horigome, and A. Takata, "Super dragon: A 10-m-long-coupled tendon-driven articulated manipulator," *IEEE Robotics and Automation Letters*, vol. 4, no. 2, pp. 934–941, April 2019.

[5] D. Keller, Y. Perrot, L. Gargiulo, J. P. Friconneau, V. Bruno, R. Le, B. Soler, M. Itchah, D. Ponsort, P. Chambaud, J. Bonnemason, S. Lamy, and Y. Measson, "Demonstration of an iter relevant remote handling equipment for tokamak close inspection," in *2008 IEEE/RSJ International Conference on Intelligent Robots and Systems*, Sep. 2008, pp. 1495–1500.

[6] Y. Perrot, L. Gargiulo, M. Houry, N. Kammerer, D. Keller, Y. Measson, G. Piolain, and A. Verney, "Long-reach articulated robots for inspection and mini-invasive interventions in hazardous environments: Recent robotics research, qualification testing, and tool developments," *Journal of Field Robotics*, vol. 29, no. 1, pp. 175–185, 2 2012. [Online]. Available: https://doi.org/10.1002/rob.20422

[7] G. Endo, H. Yamada, A. Yajima, M. Ogata, and S. Hirose, "A passive weight compensation mechanism with a non-circular pulley and a spring," in *2010 IEEE International Conference on Robotics and Automation*, May 2010, pp. 3843–3848.

[8] T. Morita, F. Kuribara, Y. Shiozawa, and S. Sugano, "A novel mechanism design for gravity compensation in three dimensional space," 08 2003, pp. 163 – 168 vol.1.

[9] S. Hirose, T. Ishii, and A. Haishi, "Float arm v: hyper-redundant manipulator with wire-driven weight-compensation mechanism," in *2003 IEEE International Conference on Robotics and Automation (Cat. No.03CH37422)*, vol. 1, Sep. 2003, pp. 368–373 vol.1.

[10] M. Takeichi, K. Suzumori, G. Endo, and H. Nabae, "Development of giacometti arm with balloon body," *IEEE Robotics and Automation Letters*, vol. 2, no. 2, pp. 951–957, April 2017.

[11] M. Takeichi, K. Suzumori, G. Endo, and H. Nabae, "Development of a 20-m-long giacometti arm with balloon body based on kinematic model with air resistance," in *2017 IEEE/RSJ International Conference on Intelligent Robots and Systems (IROS)*, 2017, pp. 2710–2716.

[12] G. Endo, T. Hagiwara, Y. Nakamura, H. Nabae, and K. Suzumori, "A proposal of super long reach articulated manipulator with gravity compensation using thrusters," in *2018 IEEE/ASME International Conference on Advanced Intelligent Mechatronics (AIM)*, July 2018, pp. 1414–1419.

[13] J. A. Silva Rico, G. Endo, S. Hirose, and H. Yamada, "Development of an actuation system based on water jet propulsion for a slim long-reach robot," *ROBOMECH Journal*, vol. 4, no. 1, p. 8, Mar 2017. [Online]. Available: https://doi.org/10.1186/s40648-017-0076-4

[14] H. Ando, Y. Ambe, A. Ishii, M. Konyo, K. Tadakuma, S. Maruyama, and S. Tadokoro, "Aerial hose type robot by water jet for fire fighting," *IEEE Robotics and Automation Letters*, vol. 3, no. 2, pp. 1128–1135, April 2018.

[15] H. Ando, Y. Ambe, T. Yamaguchi, M. Konyo, K. Tadakuma, S. Maruyama, and S. Tadokoro, "Fire fighting tactics with aerial hose-type robot "dragon firefighter"," in *2019 IEEE International Conference on Advanced Robotics and its Social Impacts (ARSO)*, Oct 2019, pp. 291–297.

[16] H. Yang, S. Park, J. Lee, J. Ahn, D. Son, and D. Lee, "Lasdra: Large-size aerial skeleton system with distributed rotor actuation," in *2018 IEEE International Conference on Robotics and Automation (ICRA)*, May 2018, pp. 7017–7023.

[17] S. Park, J. Lee, J. Ahn, M. Kim, J. Her, G. Yang, and D. Lee, "Odar: Aerial manipulation platform enabling omnidirectional wrench generation," *IEEE/ASME Transactions on Mechatronics*, vol. 23, no. 4, pp. 1907–1918, Aug 2018.

[18] S. Pan and G. Endo, "Flying watch: an attachable strength enhancement device for long-reach robotic arms," *ROBOMECH Journal*, vol. 6, no. 1, p. 5, May 2019. [Online]. Available: https://doi.org/10.1186/s40648-019-0133-2